

AD-A096 352

CALIFORNIA RESEARCH AND TECHNOLOGY INC WOODLAND HILLS

F/6 8/7

GROUND SHOCK ATTENUATION FOR DEEP BASING IN SATURATED LAYERED G-ETC(U)

JUL 80 S H SCHUSTER, K N KREYENHAGEN

DNA001-77-C-0120

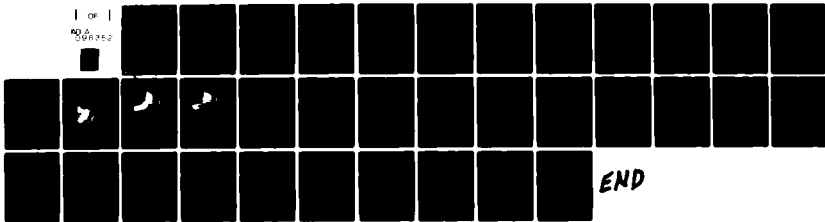
UNCLASSIFIED

CRT-3130F

DNA-5407F

NL

| OF |
NO. 096352



END

12

DNA 5407F

AD A 096352

GROUND SHOCK ATTENUATION FOR DEEP BASING IN SATURATED LAYERED GEOLOGIES

California Research & Technology, Inc.
6269 Variel Avenue
Woodland Hills, California 91367

LEVEL II

1 July 1980

Final Report for Period 1 February 1977-1 July 1980

CONTRACT No. DNA 001-77-C-0120

APPROVED FOR PUBLIC RELEASE;
DISTRIBUTION UNLIMITED.

MAR 16 1981

THIS WORK SPONSORED BY THE DEFENSE NUCLEAR AGENCY
UNDER RD&E RMSS CODE 8344077464 Y99OAXSC3/002 H2590D.

Prepared for
Director
DEFENSE NUCLEAR AGENCY
Washington, D. C. 20305

DBG FILE COPY

81 3 13 031

Destroy this report when it is no longer needed. Do not return to sender.

PLEASE NOTIFY THE DEFENSE NUCLEAR AGENCY,
ATTN: STTI, WASHINGTON, D.C. 20305, IF
YOUR ADDRESS IS INCORRECT, IF YOU WISH TO
BE DELETED FROM THE DISTRIBUTION LIST, OR
IF THE ADDRESSEE IS NO LONGER EMPLOYED BY
YOUR ORGANIZATION.



UNCLASSIFIED

SECURITY CLASSIFICATION OF THIS PAGE (When Data Entered)

REPORT DOCUMENTATION PAGE		READ INSTRUCTIONS BEFORE COMPLETING FORM
1. REPORT NUMBER DNA 5407F	2. GOVT ACCESSION NO. AD A096352	3. RECIPIENT'S CATALOG NUMBER
4. TITLE (and Subtitle) GROUND SHOCK ATTENUATION FOR DEEP BASING IN SATURATED LAYERED GEOLOGIES.	5. TYPE OF REPORT & PERIOD COVERED Final Report, See Report 1 Feb 77 - 1 Jul 80	6. PERFORMING ORG. REPORT NUMBER CRT-3130F
7. AUTHOR(s) S. H./Schuster and K. N./Kreyenhagen	8. CONTRACT OR GRANT NUMBER(s) DNA 001-77-C-0120 <i>see</i>	
9. PERFORMING ORGANIZATION NAME AND ADDRESS California Research & Technology, Inc. 6269 Variel Avenue Woodland Hills, California 91367	10. PROGRAM ELEMENT, PROJECT, TASK AREA & WORK UNIT NUMBERS Subtask <i>17</i> Y99QAXSC370-02	
11. CONTROLLING OFFICE NAME AND ADDRESS Director Defense Nuclear Agency Washington, D.C. 20305	12. REPORT DATE 1 Jul 80	13. NUMBER OF PAGES 34 <i>1-37</i>
14. MONITORING AGENCY NAME & ADDRESS (if different from Controlling Office)	15. SECURITY CLASS. (of this report) UNCLASSIFIED	15a. DECLASSIFICATION/DOWNGRADING SCHEDULE
16. DISTRIBUTION STATEMENT (of this Report) Approved for public release; distribution unlimited.		
17. DISTRIBUTION STATEMENT (of the abstract entered in Block 20, if different from Report)		
18. SUPPLEMENTARY NOTES This work sponsored by the Defense Nuclear Agency under RDT&E RMSS Code B344077464 Y99QAXSC37002 H2590D.		
19. KEY WORDS (Continue on reverse side if necessary and identify by block number) deep basing finite difference ground motions numerical analysis diffraction stratigraphic layering		
20. ABSTRACT (Continue on reverse side if necessary and identify by block number) Finite difference code calculations were conducted using the 2-D CRALE code to determine if distinct stratigraphic layering would substantially contribute to attenuation of stresses and motions at depth beneath large nuclear bursts over saturated geologies. Three geologies were examined: In Case 1, there were five distinct layers of soft rocks above the bedrock at 2300 ft. In Case 2, layers were homogenized to eliminate diffraction at interfaces. Case 3 was the same as Case 1, but with 1% hysteretic compaction in layers above the bedrock to simulate air entrainment. The burst was represented as a shallow-buried		

DD FORM 1473 EDITION OF 1 NOV 65 IS OBSOLETE

UNCLASSIFIED

SECURITY CLASSIFICATION OF THIS PAGE (When Data Entered)

UNCLASSIFIED

SECURITY CLASSIFICATION OF THIS PAGE (When Data Entered)

20. ABSTRACT (Continued)

isothermal sphere containing 7.5 Mt of energy.

The results show only minor differences between waveforms and peak stresses for the three cases. Peak stresses attenuated approximately as the square of the depth, i.e., $\sigma_{\max} \propto D^{-2}$ (similar to attenuation observed

in hard rock). Layering in media above the bedrock (Case 1) reduce stresses in the bedrock by only 10-15% (as compared with the homogenized media in Case 2). In the three cases, stresses above 1.5 kb were experienced to depths between about 3200 and 3800 ft.

It is concluded that the effects of typical layering in saturated sedimentary soft rock layers will not substantially reduce peak stresses beneath near-surface bursts. Deep base facilities in such geologies would probably need to be placed at depths equivalent to those required in hard rock.

UNCLASSIFIED

TABLE OF CONTENTS

<u>Section</u>		<u>Page</u>
	LIST OF ILLUSTRATIONS	2
1	INTRODUCTION AND SUMMARY.	3
	1.1 BACKGROUND	3
2	APPROACH.	5
	2.1 GEOLOGIC PROFILES.	5
	2.2 SOURCE CONDITIONS.	5
	2.3 NUMERICAL METHOD	8
3	RESULTS	9
	3.1 DEVELOPMENT OF GROUND MOTIONS.	9
	3.2 STRESS, VELOCITY, AND DISPLACEMENT WAVEFORMS BENEATH BURST.	13
4	CONCLUSIONS	20
	REFERENCES.	22
	APPENDIX - GEOLOGY AND MATERIAL MODELING.	23

Accession For	
Title	
Author	
Date	
Project	
Notes	
A	

LIST OF ILLUSTRATIONS

<u>Figure</u>	<u>Page</u>
1 Geologic Profiles for Numerical Solutions	6
2 Material Properties Profiles used in Numerical Solutions	7
3 Velocity Vector Field at 78 msec in Case 1 - Basic Layered Profile, Totally Saturated.	10
4 Velocity Vector Field at 123 msec in Case 1 - Basic Layered Profile, Totally Saturated.	11
5 Velocity Vector Field at 113 msec in Case 2 - Homogenized Layers between 410 ft and 2300 ft	12
6 Stress, Velocity, and Displacement Time Histories Near Axis at 1300 ft Depth (395 m).	14
7 Stress, Velocity, and Displacement Time Histories Near Axis at 2460 ft Depth (750 m) in the Bedrock	15
8 Peak On-Axis Stress vs Depth.	16
9 Peak Stress Contours.	18
10 Peak On-Axis Displacement vs Depth.	19
A-1 Stress Profile at 2130 ft (650 m) Obtained from 1-D Spherical Analyses to Assess Effects of Homogenized Properties on Waveforms Incident to the Bedrock Interface	26

SECTION 1.

INTRODUCTION AND SUMMARY

1.1 BACKGROUND

Deep basing concepts attempt to increase the survivability of strategic reserve forces or command systems by placing such facilities several thousand feet underground, depending on attenuation in the geologic media to reduce the ground shock from nuclear bursts on or near the surface to acceptable levels.

In homogeneous media, the depths required to attenuate peak over stresses to a given level have been estimated by Cooper¹ from underground test data:

$$\text{Hard rock: } W^{1/3} \sigma_{\max}^{1/2} \leq D \leq 2W^{1/3} \sigma_{\max}^{1/2} \quad (1)$$

$$\text{Soft rock: } 0.4W^{1/3} \sigma_{\max}^{1/2} \leq D \leq 9.8W^{1/3} \sigma_{\max}^{1/2} \quad (2)$$

where

W = yield (Mt) of a shallow-buried burst

σ_{\max} = peak over stress level (kb)

D = depth (kft)

For a shallow burst of $W = 7.5$ Mt and a peak over stress level of $\sigma_{\max} = 1.5$ kb, the estimated depths are:

In hard rock: $D = 1600-3200$ ft (500-1000 m)

In soft, dry rock: $D = 650-1300$ ft (200-400 m)

An optimum deep basing geology might consist of a relatively thin hard rock surface layer (to discourage use of earth penetrators), over a thick, fairly uniform layer of dry, porous soft

rock (to provide rapid shock attenuation), over a hard bedrock (to provide structural resistance). A geology of this nature can be found, for example, in Idaho and eastern Oregon, where a basalt flow overlies a thick pumice layer over a hard bedrock². Suitable geologies without the surface rock are common in the Southwest.

The occurrence of dry, porous sites with promising shock attenuation characteristics (with or without the surface rock) does not, however, assure that such sites are available nor desirable for deep basing. Alternative geologies may be preferable for operational or other practical reasons. The existence of support facilities, for example, may make it desirable to locate deep base facilities at or near existing Minuteman sites, providing that the deep facility is survivable in Minuteman geologies. These typically consist of multiple layers of shales and softer sedimentary rocks over a hard basement at 2000-4000 feet (600-1200 m). Unfortunately, the water table is generally shallow, and ground shock attenuation through saturated porous media is more gradual than in dry porous media. There is some question whether Minuteman geologies, or any other saturated porous geologies, are practical for deep basing, since stresses sufficient to destroy structures (say $\sigma_{\max} > 1.5 \text{ kb}$) may be experienced to unacceptably large depths.

The distinct stratigraphic layering at typical Minuteman sites, however, may provide an additional mechanism to reduce the stresses at depths. There are fairly large impedance mismatches between layers which will produce some lateral diffraction of stress waves, leading to more rapid stress wave attenuation with depth. Whether or not the degree of diffractive attenuation in such geologies will be sufficient to reduce the ground shock environment at practical depths to tolerable levels is the key technical question addressed herein.

SECTION 2.

APPROACH

2.1 GEOLOGIC PROFILES

Three finite difference calculations were performed of the stress wave propagation and ground motions beneath a 7.5 Mt shallow-buried burst, using the geologic profiles in Figure 1, and the properties in Figure 2. The detailed material models are described in the Appendix. The basic profile (Case 1) contains several layers of saturated, soft sedimentary rock above a hard bedrock. Its dimensions and properties were constructed using data provided by J. Zelasko of Waterways Experiment Station³.

In Case 1, the major geologic layers were separately defined in the computational grid, and all the layers were totally saturated (i.e., there was no air-filled porosity).

In Case 2, layers between the surface layer and the bedrock were homogenized into a single layer having weighted-average properties. Comparisons between the layered vs homogenized models in Case 1 vs Case 2 permit assessment of the effects of reflection and diffraction processes at interfaces upon stress attenuation beneath the burst.

Even in nominally-saturated porous media, there is probably a small amount of air entrapped in cracks and pores. To assess the possible importance of such air-filled porosity, hysteretic compaction in the soft rock layers above the bedrock was specified in Case 3.

2.2 SOURCE CONDITIONS

In selecting the burst condition, it was assumed that a 30-Mt surface burst would be a credible threat against a deep-based facility. To avoid the need for calculating the details of energy coupling from such a surface burst, it was further assumed that a

Case 1. Basic profile of layered, saturated, soft sedimentary rocks over bedrock. Layers were explicitly modeled.

Case 2. Same geology but layers 2-4 were homogenized using weighted average properties.

Case 3. Same as Case 1, but with 1% hysteretic compaction in all layers above bedrock to simulate air-filled voids.

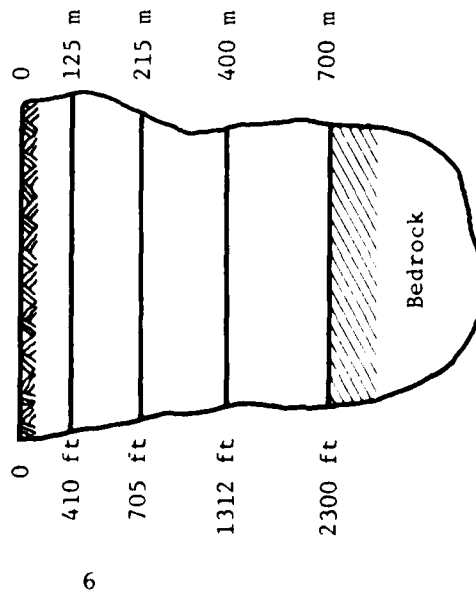


Figure 1. Geologic Profiles for Numerical Solutions.

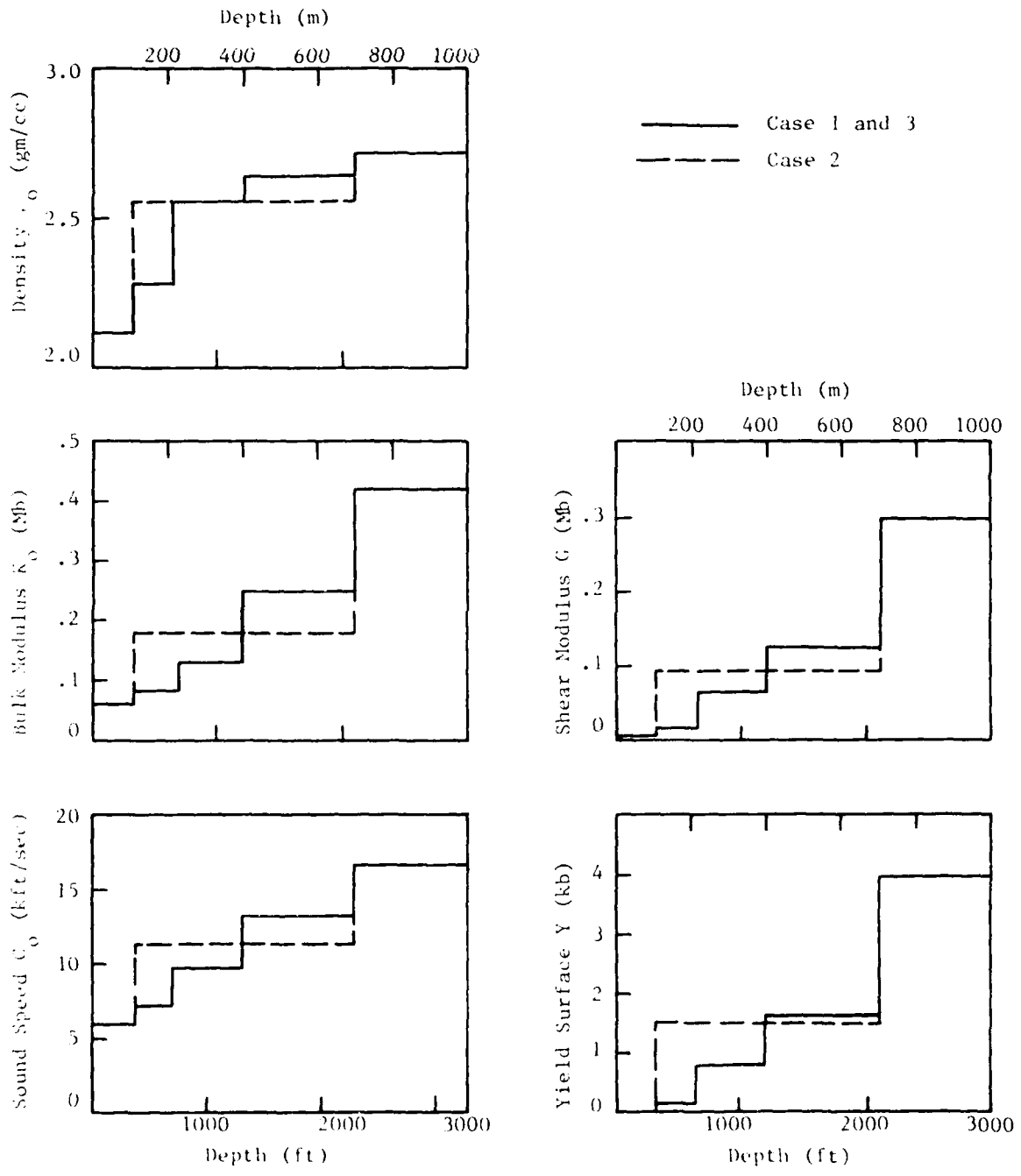


Figure 2. Material Properties Profiles used in Numerical Simulations.

surface burst produces the same ground motion effects as a shallow-buried burst of 1/4th the yield². The source was therefore represented as 7.5 Mt of energy uniformly distributed in a 6-m radius sphere of Layer 1 material centered 10 m below the surface. This gave an initial pressure of 140 Mb. The effects of airblast on the surface were modeled by application of the Brode overpressure function to the upper boundary of the grid, using $W = 7.5$ Mt.

2.3 NUMERICAL METHOD

The three 2-D problems were run using the CRALE (California Research Arbitrary Lagrangian-Eulerian) code, an axisymmetric finite-differencing time-marching program. In this code, the grid motion algorithm allows the user to rezone the grid points *each cycle* in order to maintain reasonable zone sizes and shapes. For the problems in this study, the initially vertical lines were required to remain vertical. The initially horizontal interfaces separating layers were treated as Lagrangian grid lines, i.e., the grid lines were displaced as the interfaces deformed. Between these interfaces, the initially horizontal grid lines moved so as to remain equally spaced. Thus, material was transported across grid lines within each layer, but not across interfaces. Material at the ground surface moving upward at high velocity was allowed to pass through the top of the grid.

SECTION 3.

RESULTS

3.1 DEVELOPMENT OF GROUND MOTIONS

Development of the ground motions is illustrated by the velocity vector fields in Case 1 at 78 and 123 msec after the burst. By 78 msec (Figure 3), the main shock front is approximately 1000 ft from the source and the peak stress is about 7.5 kb. At this time, the layering does not appear to significantly affect the propagation of the diverging wave. By 123 msec (Figure 4), the main shock has reached a depth of about 1500 ft and the peak stress has attenuated to about 4 kb. The layering is still not significantly perturbing the shock front, but there is some rotation of particle velocities behind the shock just below the 705 ft interface, due to differences in the yield condition in materials above and below that interface.

The velocity field at 113 msec for Case 2, in which layers between 410 ft and the bedrock at 2300 ft were homogenized, show a very pronounced interface effect at 410 ft depth (Figure 5). This is because the homogenization of properties for layers below 410 ft led to a relatively large mismatch of properties across that interface (see Figure 2). In particular, stresses were still sufficient to cause yielding above that interface (where the Mises yield surface, $Y = 0.1$ kb), but were insufficient to produce yielding in the much stronger material below the interface (in which $Y = 1.5$ kb). The result is a discontinuity in particle velocities. In addition, the substantially higher wave velocity beneath the interface led to the outrunning condition which is evident in Figure 5. These phenomena at the shallow interface did not, however, substantially affect the stresses and ground motions at depth.

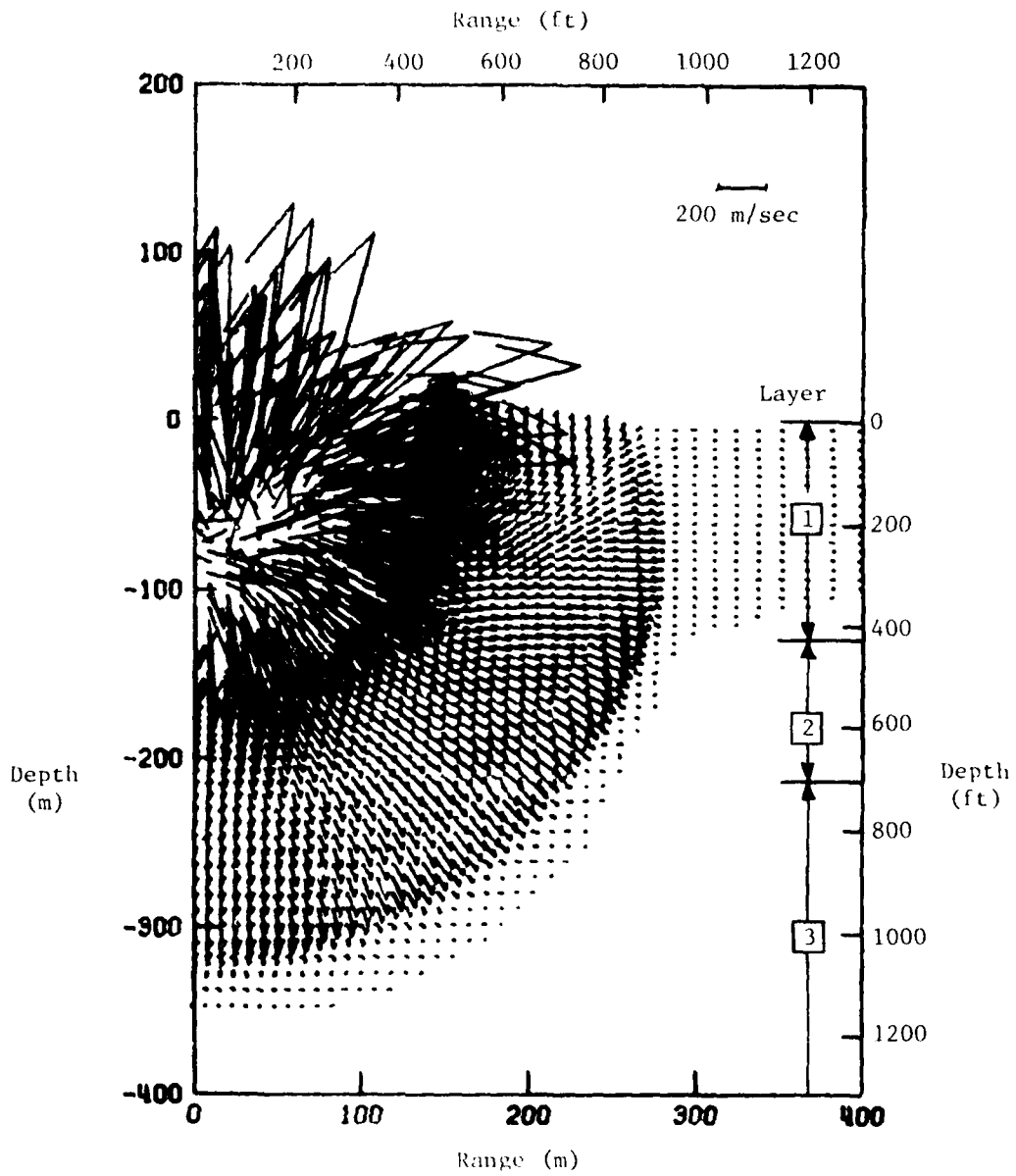


Figure 3. Velocity Vector Field at 78 msec in Case 1 - Basic Layered Profile, Totally Saturated

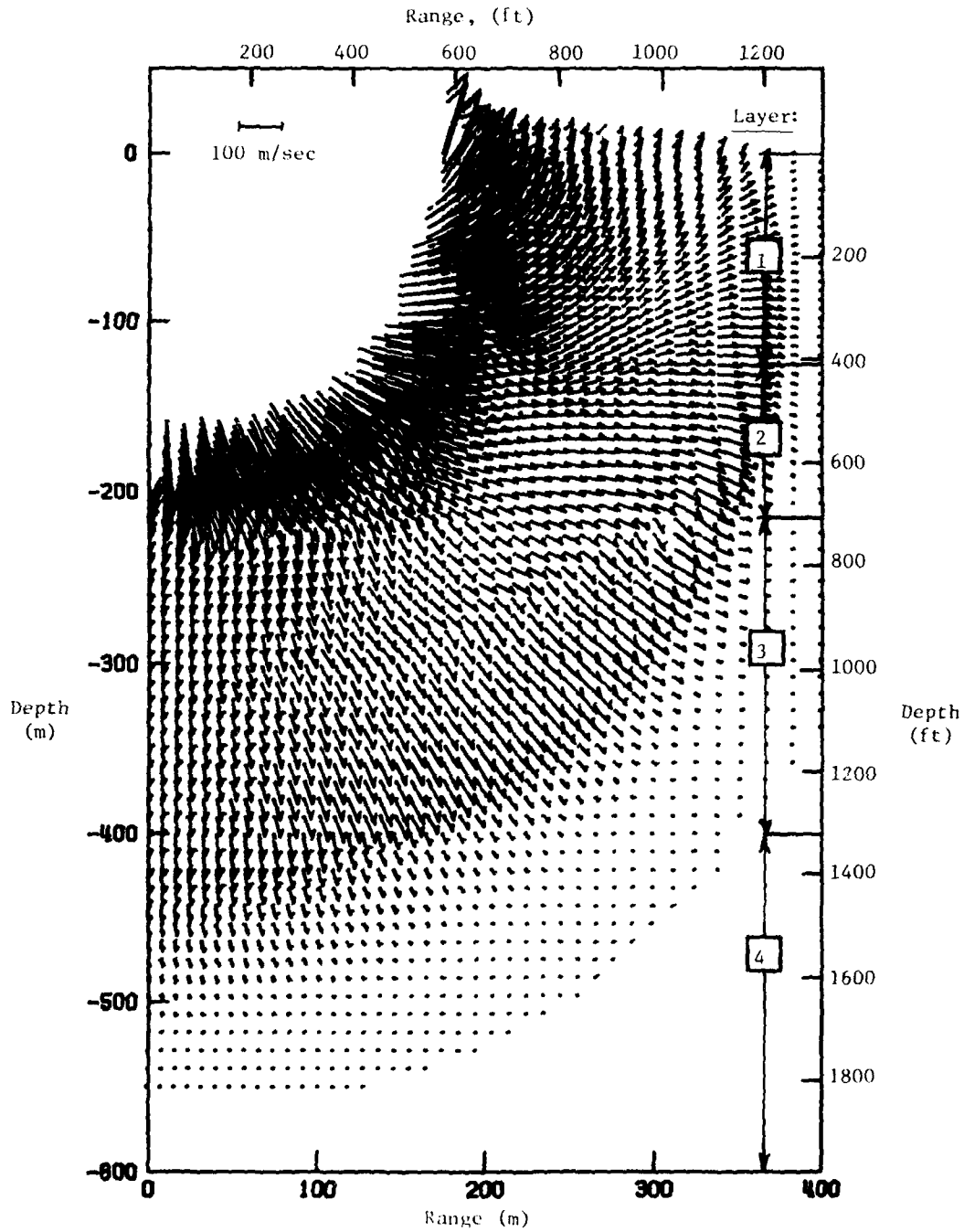


Figure 4. Velocity Vector Field at 123 msec in Case 1 - Basic Layered Profile, Totally Saturated. (Vectors in vaporized region near source are suppressed.)

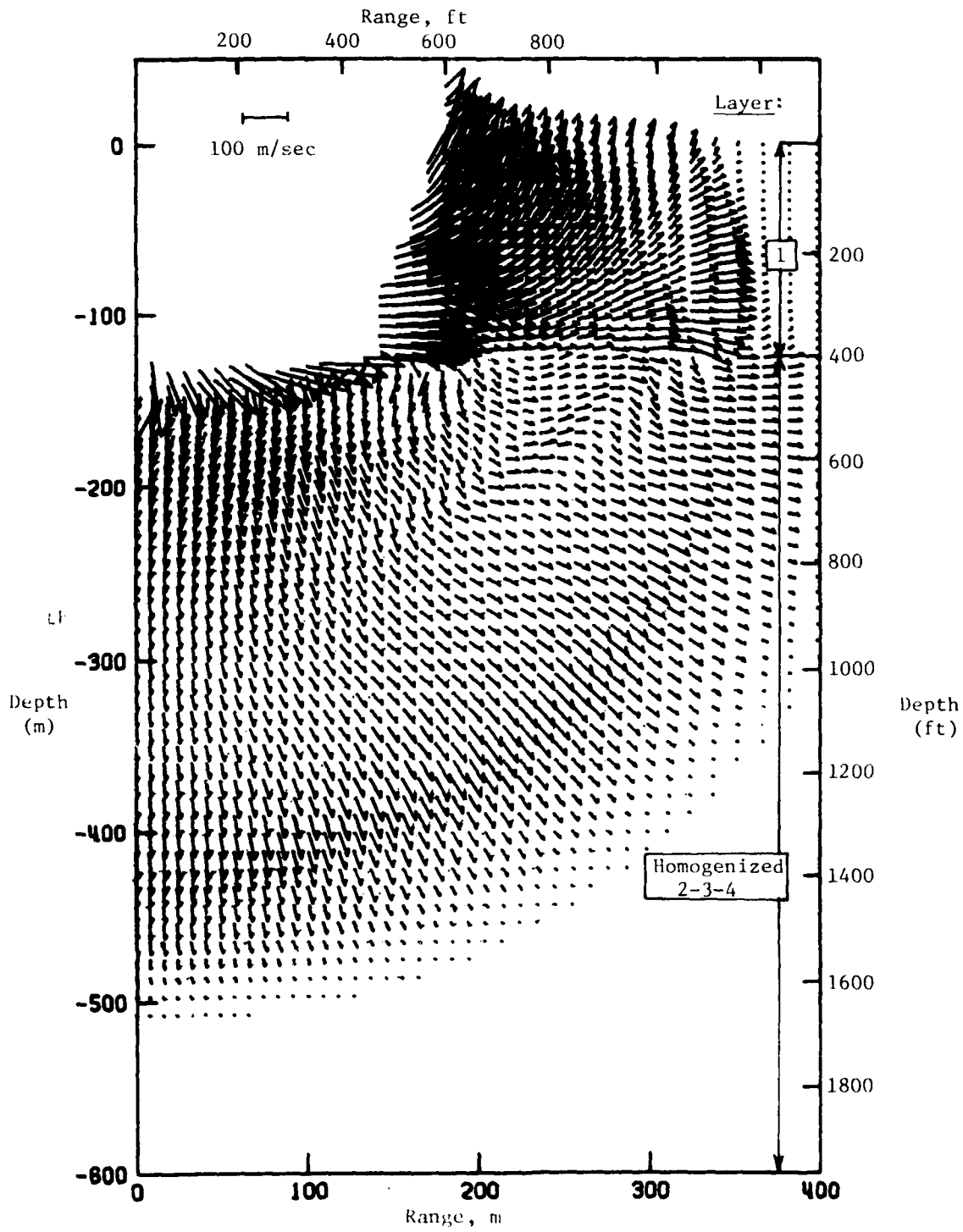


Figure 5. Velocity Vector Field at 113 msec in Case 2 - Homogenized Layers between 410 ft and 2300 ft. (Vectors in vaporized region near source are suppressed.)

3.2 STRESS, VELOCITY, AND DISPLACEMENT WAVEFORMS BENEATH BURST

The similarity of basic ground motions beneath the burst in the three geologic profile cases is illustrated by comparing the near-axis stress, velocity, and displacement histories in the soft rock at 1300 ft depth and in the bedrock at 2460 ft depth.

At the station in the soft rock (Figure 6), there are only minor differences between the waveforms. At the deeper station (Figure 7), the effects of the large mismatch of properties at the bedrock interface in the homogenized profile (Case 2) results in a sharper, somewhat stronger stress pulse entering the bedrock. Peak displacements in the homogenized profile, by contrast, are somewhat lower than in the corresponding layered profile (Case 1). In the layered geology with 1% hysteretic compaction (Case 3), stresses and velocities drop more quickly, due to the higher velocity of relief waves in the hysteretic model. Displacements in Case 3 are therefore smaller.

Peak stresses vs depth for near-axis locations are shown in Figure 8. *Differences between the three cases are relatively small at all depths.* At depths down to the bedrock interface at 2300 ft, the calculated stresses attenuate approximately as the square of the depth, i.e., $\sigma_{\max} \propto D^{-2}$. In the layered geology (Case 1), stresses incident upon the bedrock are slightly *higher* than in the homogenized geology (Case 2), but the smoother match of properties across the softrock-bedrock interface in Case 1 results in lower stresses entering the bedrock, and this difference persists. Thus layering in media above the bedrock (as in Case 1) reduces the stresses in the bedrock (as compared with homogeneous media), but only by 10-15%.

The introduction of 1% hysteretic compaction to account for a small degree of air-filled porosity does not significantly affect the peak stress vs depth.

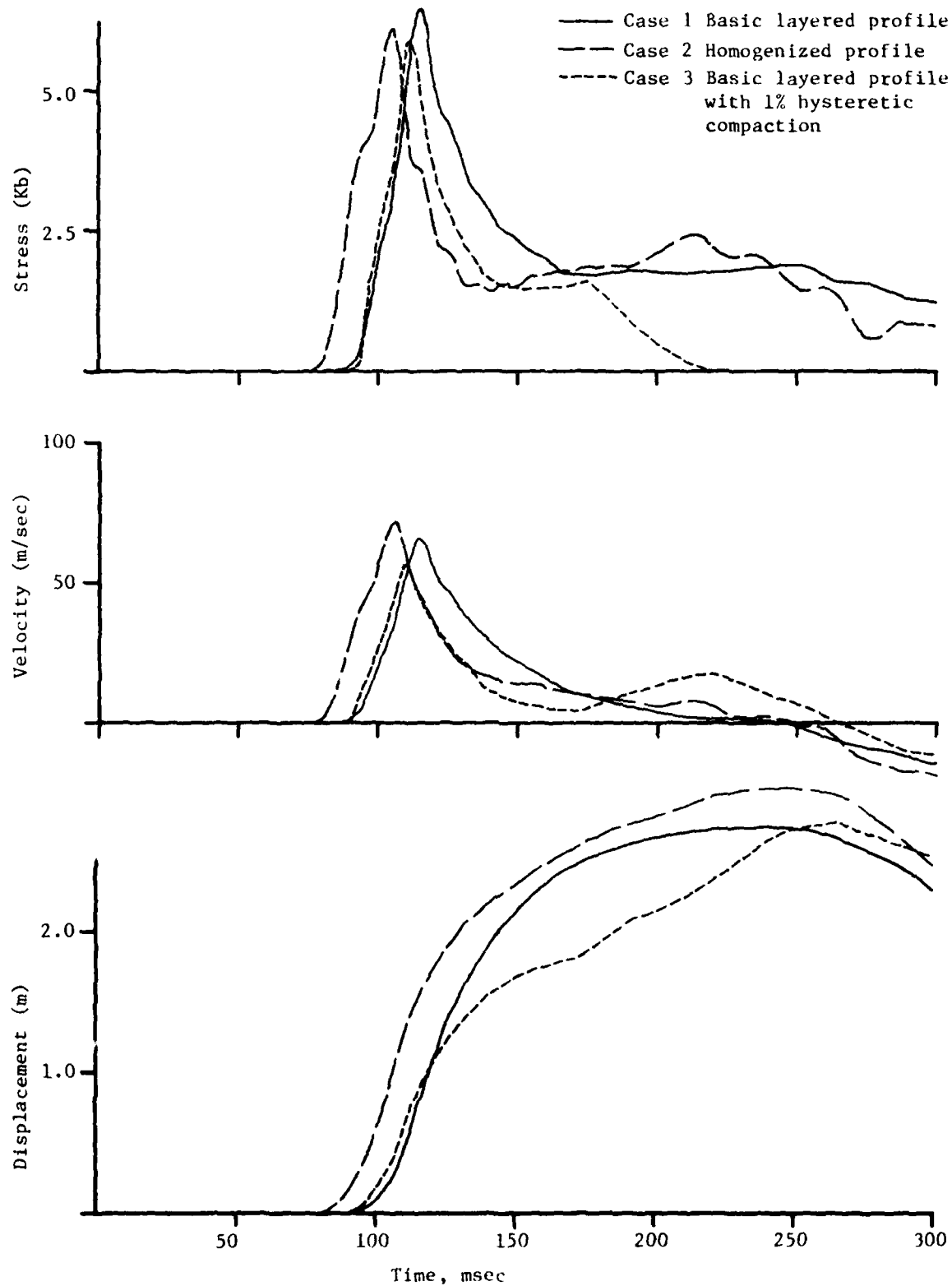


Figure 6. Stress, Velocity, and Displacement Time Histories Near Axis at 1300 ft Depth (395 m).

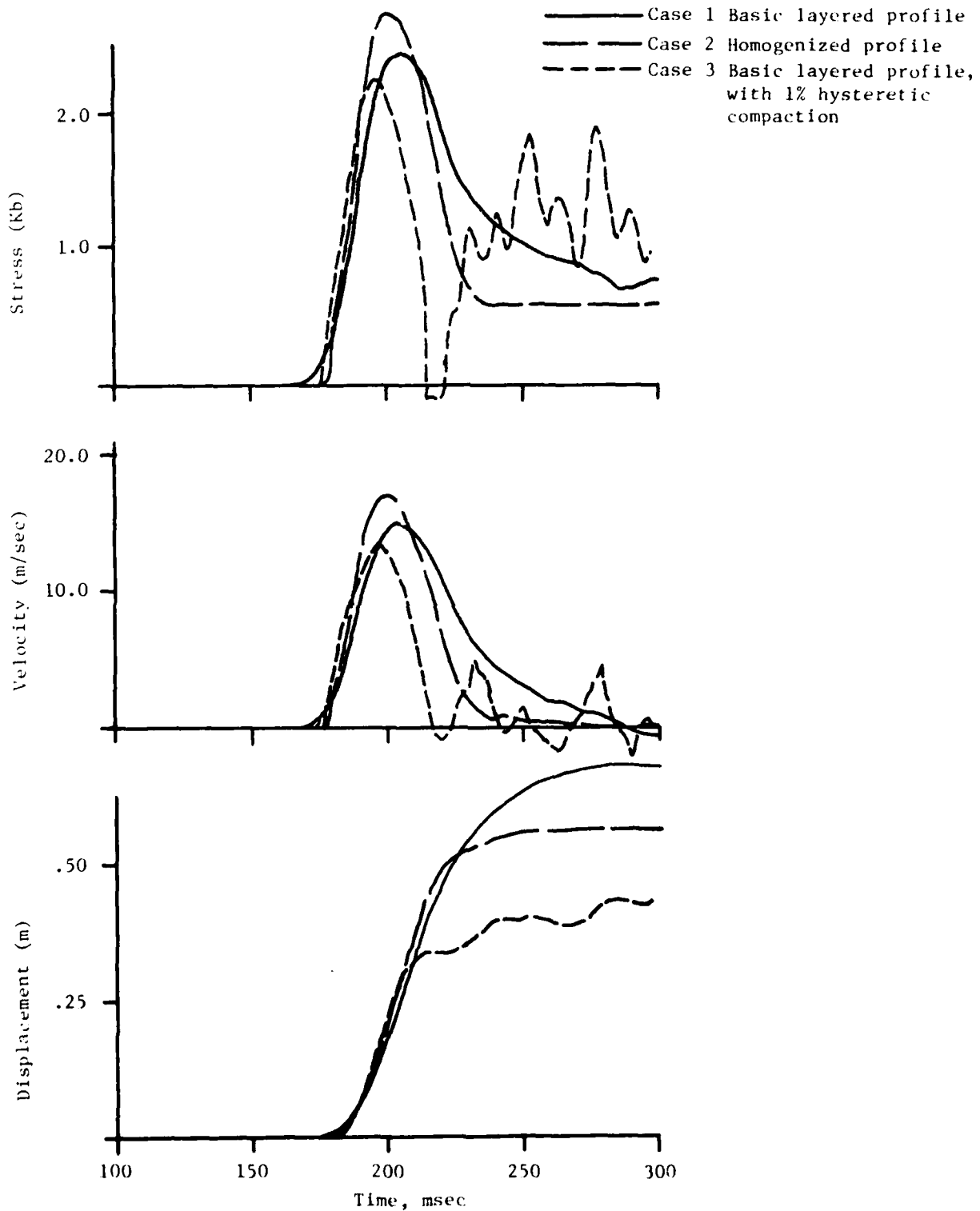


Figure 7. Stress, Velocity and Displacement Time Histories Near Axis at 2460 ft Depth (750 m) in the Bedrock.

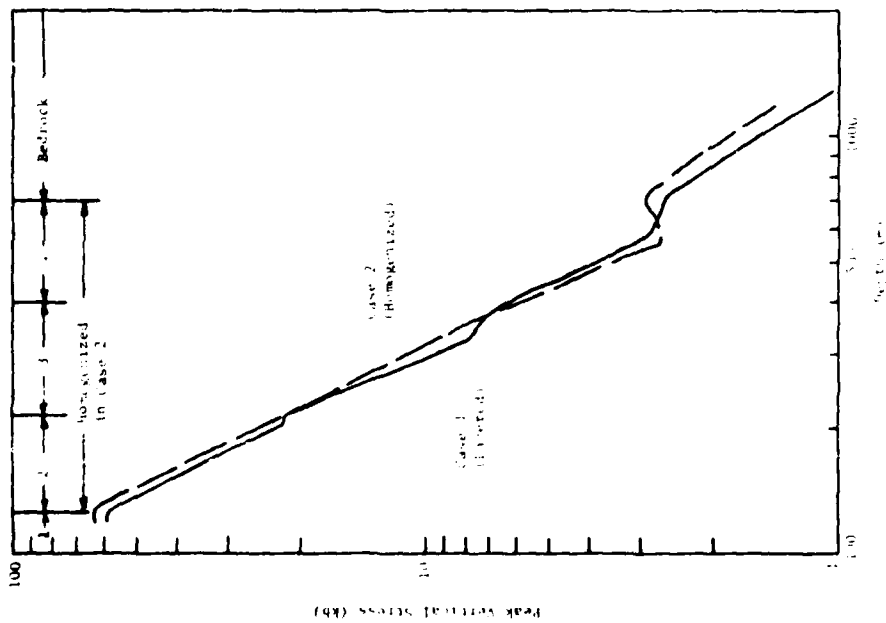
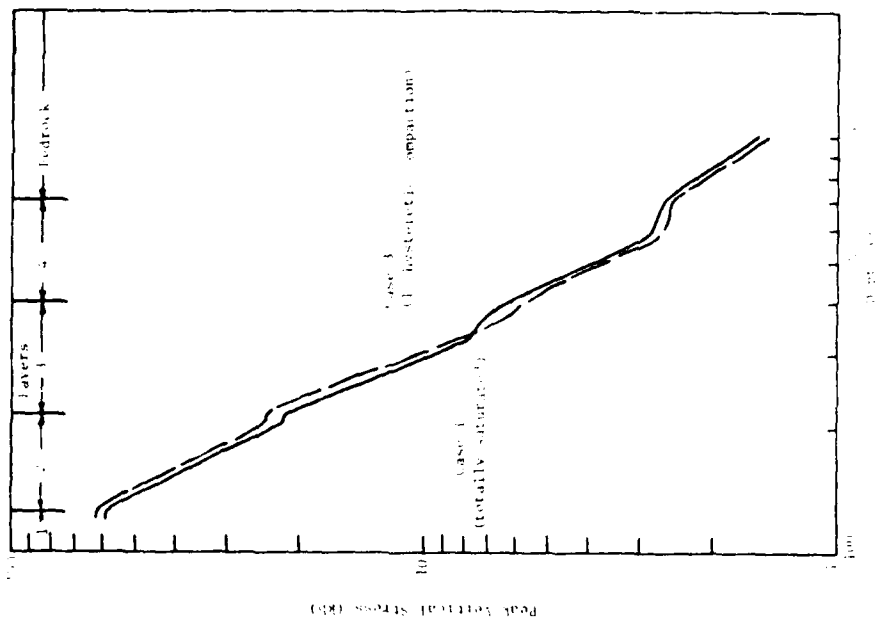


Figure 8. Peak On-Axis Stress vs Depth.

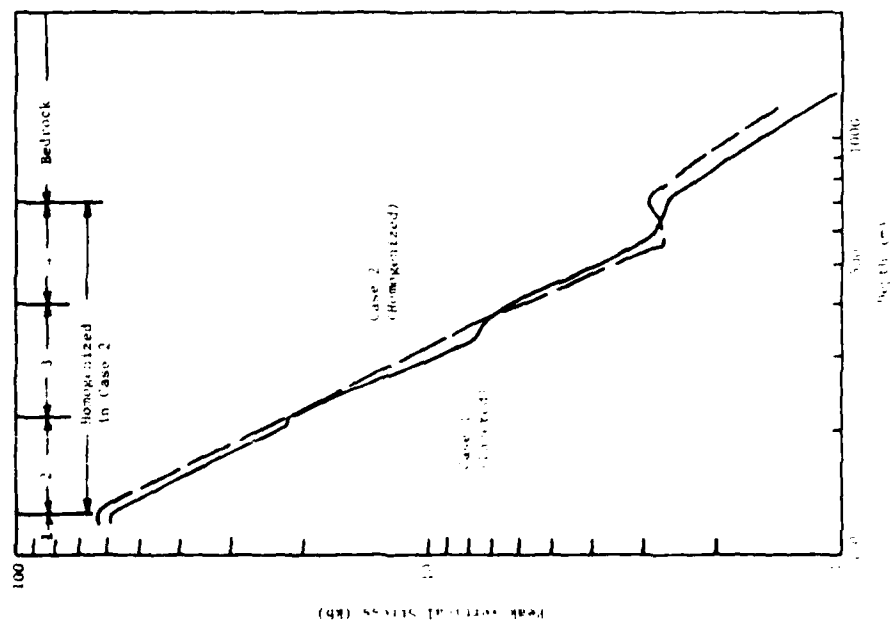
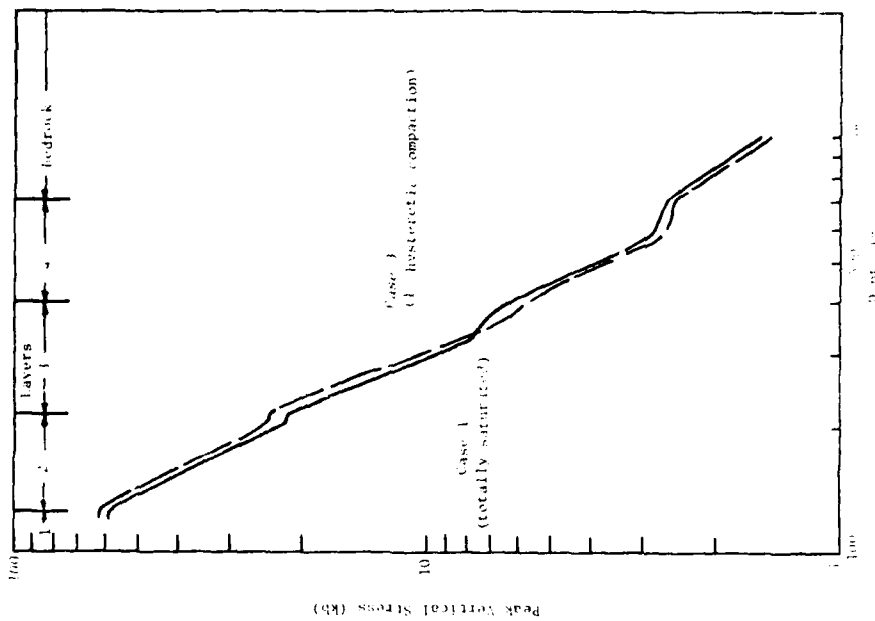


Figure 8. Peak On-Axis Stress vs Depth.

Figure 9 shows peak stress contours for the three cases. Comparison of Cases 1 and 2 shows that layering reduces the maximum depths and ranges in the bedrock at which damaging peak stresses are experienced, but not by significant margins. For example, when there is an unlayered medium above the bedrock, 1.5 kb peak stresses are experienced to a maximum of 2705 ft depth, and to a maximum range (from the axis) in the bedrock of 1310 ft. When there is layered media above the bedrock, 1.5 kb peak stresses extend only to 3345 ft depth, and to 1150 ft range in the bedrock. With 1% hysteresis in the layered media, the maximum depth is further reduced to 3180 ft, and the maximum range in the bedrock to 1000 ft.

Figure 10 shows peak displacements. The differences are small, except in the 1% hysteretic geology (Case 3), where much smaller displacements occur in the bedrock. This is because the unloading arrives relatively sooner in the hysteretic geology, thereby shortening the downward pulse.

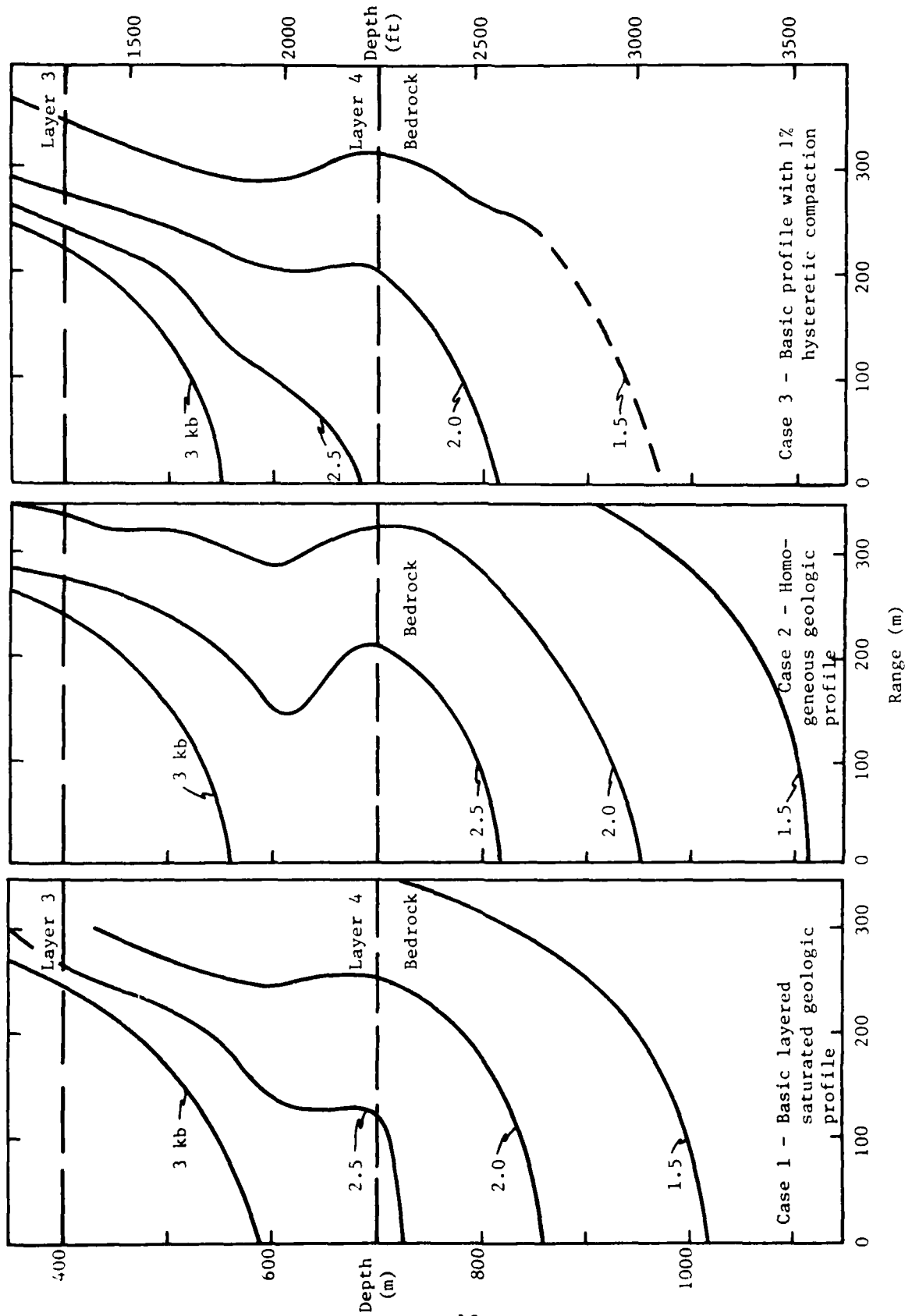


Figure 9. Peak Stress Contours

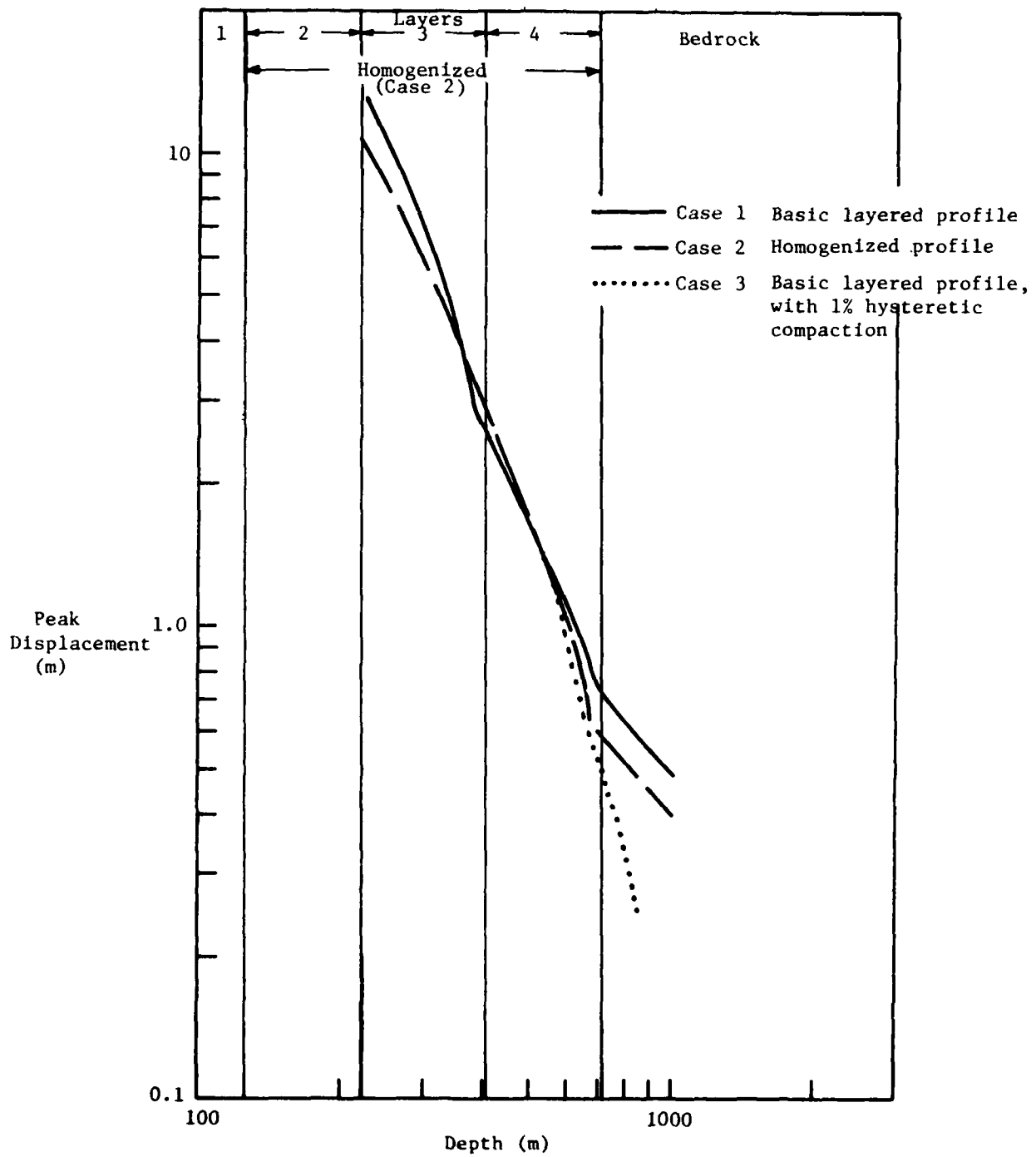
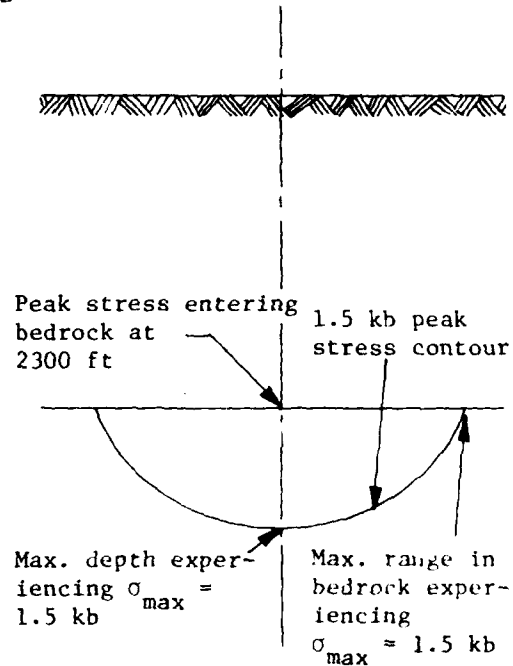


Figure 10. Peak On-Axis Displacement vs Depth.

SECTION 4.

CONCLUSIONS

The three parameters defined in the sketch are used to summarize key findings of the analyses in the following tabulation.



	Peak Stress Entering Bedrock	Max. Depth Experiencing $\sigma_{max} = 1.5 \text{ kb}$	Max. Range in Bedrock Experiencing $\sigma_{max} = 1.5 \text{ kb}$
Case 1. Basic layered, saturated profile	2.6 kb	3345 ft (1020 m)	1150 ft (350 m)
Case 2. Homogenized media above bedrock	2.9 kb	3705 ft (1120 m)	1310 ft (400 m)
Case 3. Same as Case 1, but with 1% hysteretic compaction	2.4 kb	3180 ft (970 m)	1000 ft (305 m)

The *trends* seen in this tabulation are as would be expected; sedimentary layering or hysteretic compaction will indeed reduce stresses on a deep facility beneath a near-surface burst. *However, the differences are relatively small, of the order of 10-15%.*

Futhermore, the calculated maximum depths where 1.5 kb peak stresses are experienced in geologies with saturated, layered soft rocks over deep bedrock correspond roughly with the *deepest* values predicted from empirical data for stress attenuation in *hard rock* (Equation 1).

The following conclusions are drawn from these results:

1. The effects of layering, involving typical differences in properties between sedimentary, saturated soft rock layers, do not substantially reduce peak stresses beneath near-surface bursts.
2. Deep base facilities located in geologies consisting of saturated layers of sedimentary soft rock above deep bedrock (typical of Minuteman sites) would need to be placed at depths equivalent to those required in hard rock geologies.

REFERENCES

1. H. F. Cooper, Jr., "Empirical Studies of Ground Shock and Strong Motions in Rock", DNA 3245F, October 1973.
2. H. F. Cooper, C. P. Knowles, and H. Brode, R & D Associates, personal communication.
3. J. Zelasko, Waterways Experiment Station, letter of 21 March 1977 to S. H. Schuster.
4. S. H. Schuster and J. Isenberg, "Equations of State for Geologic Materials", DNA 2925Z, September 1972.

APPENDIX

GEOLOGY AND MATERIAL MODELING

Case 1. Representative Saturated Layered Geology

The dimensions and properties for the representative saturated layered profile for Case 1 in Figure 1 were constructed using data provided by J. Zelasko of Waterways Experiment Station (WES)³. Typically there are several layers at shallow depths; we chose to model these using a single homogeneous surface layer extending down to 125 m because the very strong shock waves from the burst in this region would not be significantly affected by the relatively small impedance mismatches.

The interfaces between layers were assumed to be welded.*

The soil layers and bedrock were modeled with an updated version of the Schuster-Isenberg⁴ equations of state used extensively in nuclear and chemical explosive cratering studies. Basically, the stress-energy-strain behavior is decomposed into a mean stress or pressure relationship plus the deviatoric stress tensor. The mean stress is further decomposed into two terms, i.e.,

$$P = P_s + P_v \quad (A1)$$

where P_s represents the solid or liquid phases and P_v the vapor. Hysteresis, low-energy thermal effects, and reversible solid-solid phase changes are incorporated into the calculation of P_s .

* Differential displacements across interfaces in a layered media pose separate hazards to structures which penetrate through such interfaces; this aspect of siting in layered media was not considered in the current study.

For non-hysteretic materials,

$$P_s = K_m \mu - (K_m - K_o) \mu^* (1 - e^{-\mu/\mu^*}) \quad (A2)$$

where K_o and K_m are the initial and maximum bulk moduli, μ^* is a material parameter, and

$$\mu = \frac{\rho - \rho_o}{\rho_o} = \text{excess compression}$$

The thermal energy dependence of the solid is incorporated by adding the effect of thermal expansion to μ so that it becomes $\mu + \beta E$, where β is the coefficient of thermal expansion and E the energy density. This is equivalent to the Grunisen correction used in other models, with a variable Grunisen gamma. At a solid-solid phase change, the effective μ is again altered to reflect the decrease in $dP/d\mu$. Hence μ is replaced by $\mu - \mu_\Delta$ where

$$\mu_\Delta = \delta (\mu - \mu_p) \quad (A3)$$

and δ and μ_p are phase change parameters.

The vapor term, P_v , is computed using a variable gamma-law gas,

$$P_v = (\gamma - 1) \rho E^* \quad (A4)$$

where

$$\gamma - 1 = .4 + .23 \log \rho + [.35 \log (E^*/\rho) - .464]^2 \quad (A5)$$

and E^* is an effective energy density,

$$E^* = \begin{cases} (E - E_m) \left[1 - e^{-\left(\frac{E - E_m}{E_m}\right)} \right] & E \geq E_m \\ 0 & E < E_m \end{cases} \quad (A6)$$

Incremental deviatoric stresses are computed from changes in the deviatoric strain tensor using the elastic equation

$$d\sigma'_{ij} = -2Gde'_i \quad (A7)$$

where the shear modulus G is assumed to be constant. The second invariant of the deviatoric stress tensor, $\sqrt{J_2'}$, is then compared to a von Mises type plastic yield surface, Y . If $\sqrt{J_2'}$ exceeds Y , the material has yielded and the deviatoric stresses are reduced by the standard Drucker-Prager flow rule, i.e., without volumetric strain.

Values of the constants for the materials in each layer are listed in Table A-1. To assure correctness of seismic speeds in the various layers, the constrained moduli and Poisson's Ratio provided by Zelasko were used to determine the zero pressure moduli in the equations of state. However, the bulk modulus in each layer increased exponentially with compression to a single high pressure (> 100 kbar) value consistent with the available Hugoniot data.

Case 2. Partially Homogenized Geology

For Case 2, layers 2, 3, and 4 were homogenized and given the weighted average properties for density, bulk moduli, and sound speed shown in Table A-1. To verify that these average properties would give approximately the same waveform incident to the bedrock interface at 700 m depth as the explicitly modeled layer properties used for Case 1, comparative 1-D spherical analyses were run. The results shown in Figure A1 indicate that both models produce the same nominal waveform in a spherically diverging geometry; any differences in the 2-D solutions of Cases 1 and 2 can therefore be attributed to the diffractive effects of the interface planes.

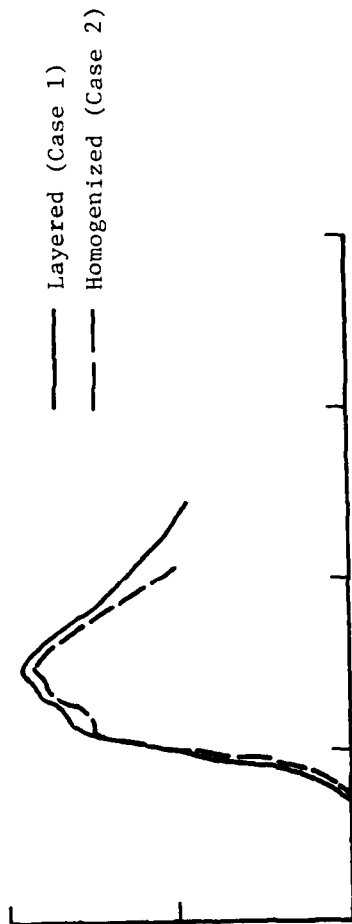


Figure A-1. Stress Profile at 2130 ft (650 m) Obtained from 1-D Spherical Analyses to Assess Effects of Homogenized Properties on Waveforms Incident to the Bedrock Interface.

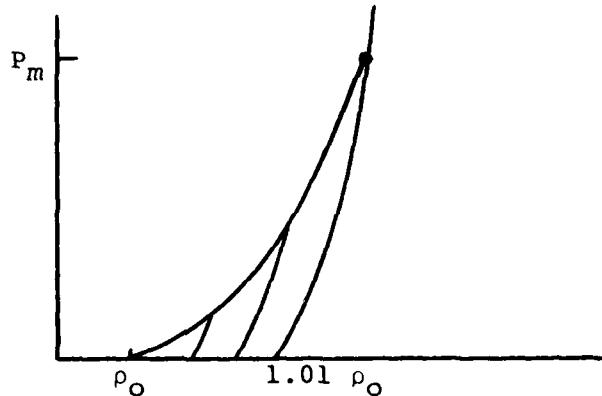
TABLE A-1. EQUATIONS OF STATE CONSTANTS

Parameter	Symbol	Units	Case 1				Bedrock	Case 2 Combined
			1	2	3	4		
Layer	Depth (m)	Depth (ft)	125-215	215-400	400-700	700-2000	2-3-4 125-700 410-2300	
Initial Density	ρ_0	gm/cc	2.11	2.28	2.56	2.72	2.56	
Initial Bulk Modulus	K_0	Mb	.06	.08	.13	.42	.18	
Maximum Bulk Modulus	K_m	Mb	.4	.4	.4	.42	.4	
* Initial Sound Speed	C_0	ft/sec	.2	.2	.2	.2	.2	
Coefficient of Thermal Expansion	β	cc/(cc-Eu)*	5,890	7,100	9,545	13,030	11,230	
Phase Change Parameters	H_p δ		3.0	3.0	3.0	3.0	3.0	
Minimum Energy for P_y	E_m	Eu	.6588	.5351	.3672	.2868	.3672	
Shear Modulus	G	Mb	1.6746	1.5439	1.3285	1.2669	1.3285	
Plastic von Mises Limit	Y	Mb	.02	.02	.02	.02	.02	
Unloading Bulk Modulus (P=0)	K_0'	Mb	.0008	.0008	.0008	.0016	.0015	
Minimum Loading Pressure to remove all air-filled porosity	P_m	Mb	.128	.124	.184	.280	---	
			.003	.0045	.0104	.0519	---	

*1 Eu = 1 energy unit = 10¹² ergs

Case 3. Near-Saturated Layered Geology

Even in nominally-saturated porous media, there is probably a small amount of air entrapped in cracks and pores. To assess the possible importance of such air-filled porosity, 1% hysteretic compaction in Layers 1-4 was allowed in Case 3. To retain the basic characteristics of the Case 1 materials, the loading moduli and hence the sound speeds were not changed. Upon unloading, however, K_0 in Equation A2 was replaced by K'_0 (Table A-1) so that the effective modulus was much higher and the material returned to zero pressure at a density up to 1% higher than initial density, as shown in this sketch.



The value of P_m , the minimum pressure required to collapse all of the air-filled voids increased with the depth of the layers (Table A-1) to be consistent with the increase in the initial loading moduli.

DEPARTMENT OF DEFENSE

Assistant to the Secretary of Defense
Atomic Energy

ATTN: Executive Assistant

Defense Advanced Rsch Proj Agency

ATTN: TIO

Defense Intelligence Agency

ATTN: DB-4C2

ATTN: RDS-3A

Defense Nuclear Agency

ATTN: RAEV

ATTN: STNA

3 cy ATTN: SPSS

4 cy ATTN: TITL

Defense Technical Information Center

12 cy ATTN: DD

Field Command

Defense Nuclear Agency

ATTN: FCTMOF

ATTN: FCPR

Field Command

Defense Nuclear Agency

Greenmore Branch

ATTN: FCPRL

Field Command Test Directorate

Test Construction Division

Defense Nuclear Agency

2 cy ATTN: FCTC, J. Lacombe

Joint Strat Tgt Planning Staff

ATTN: NRI-STINFO Library

ATTN: JLA

Undersecretary of Def for Rsch & Engrg

ATTN: Strategic & Space Sys (OS)

DEPARTMENT OF THE ARMY

Chief of Engineers

Department of the Army

ATTN: DAEN-MCE-D

ATTN: DAEN-RDL

Construction Engineering Rsch Lab

Department of the Army

ATTN: CERL-SOI-L

Harry Diamond Laboratories

Department of the Army

ATTN: DELHD-N-P

U.S. Army Ballistic Research Labs

ATTN: DRDAR-BLV

ATTN: DRDAR-BLT, J. Keefer

ATTN: DRDAR-TSB-S

ATTN: DRDAR-BLT, W. Taylor

U.S. Army Communications Command

ATTN: Technical Reference Division

DEPARTMENT OF THE ARMY (Continued)

U.S. Army Concepts Analysis Agency

ATTN: CSSA-ADL

U.S. Army Engineer Center

ATTN: DT-RC

U.S. Army Engineer Dist, Omaha

ATTN: MROED-D, C. Distefano

U.S. Army Engineer Div, Huntsville

ATTN: HNEED-SR

3 cy ATTN: C. Huang

U.S. Army Engineer Div, Ohio River

ATTN: ORDAS-L

U.S. Army Engr Waterways Exper Station

ATTN: WESSS, J. Ballard

ATTN: Library

ATTN: WESSD, J. Jackson

ATTN: WESSE, I. Ingram

ATTN: WESSA, W. Flathau

ATTN: J. Day

ATTN: J. Drake

ATTN: P. Mlakar

U.S. Army Nuclear & Chemical Agency

ATTN: Library

DEPARTMENT OF THE NAVY

Dir Cmd Control Planning & Program Div

Department of the Navy

ATTN: OP-943

Naval Construction Battalion Center

ATTN: Code 151, R. Odello

ATTN: Code 151, S. Takahashi

ATTN: Code 108A

ATTN: Code 151, W. Shaw

ATTN: Code 144, H. Haynes

Naval Electronic Systems Command

ATTN: PME 117-211, B. Kruger

Naval Postgraduate School

ATTN: Code 1424 Library

Naval Research Laboratory

ATTN: Code 2627

Naval Surface Weapons Center

ATTN: Tech Library & Info Svcs Br

Naval War College

ATTN: Code E-11

Strategic Systems Project Office

Department of the Navy

ATTN: NSP-43

DEPARTMENT OF THE AIR FORCE

Air Force Institute of Technology

ATTN: Library

DISTRIBUTION LIST

DEPARTMENT OF THE AIR FORCE (Continued)

Air Force Weapons Laboratory
Air Force Systems Command
ATTN: NIYW, D. Payton
ATTN: NTE, M. Plamondon
ATTN: SUL

Assistant Chief of Staff
Studies & Analyses
Department of the Air Force
ATTN: AF/SASM

Ballistic Missile Office
Air Force Systems Command
ATTN: MHHH
ATTN: MNN

Deputy Chief of Staff
Operations Plans and Readiness
Department of the Air Force
ATTN: AFXODC

Deputy Chief of Staff
Research, Development, & Acq
Department of the Air Force
ATTN: AFRDQI

Foreign Technology Division
Air Force Systems Command
ATTN: NIIS Library

Strategic Air Command
Department of the Air Force
ATTN: NRI-STINFO Library
ATTN: XPFS

OTHER GOVERNMENT AGENCIES

Central Intelligence Agency
ATTN: OSWR/NED

Department of the Interior
Bureau of Mines
ATTN: Tech Lib

Department of the Interior
Geological Survey
ATTN: W. Iwenhofel
ATTN: R. Carroll

Department of the Interior
Geological Survey
ATTN: D. Roddy

DEPARTMENT OF ENERGY CONTRACTORS

Lawrence Livermore National Lab
ATTN: Technical Info Dept Library
ATTN: 4-21, D. Oakley
ATTN: H. Heard

Los Alamos National Scientific Lab
ATTN: B. Killian
ATTN: L. Germaine
ATTN: G. Johnson
ATTN: M, 364

Sandia National Laboratory
ATTN: Central Research Library

DEPARTMENT OF ENERGY CONTRACTORS (Continued)

Sandia National Laboratories
Livermore National Laboratory
ATTN: Library & Security Class Div

Sandia National Lab
ATTN: Code 3141
ATTN: L. Hill

DEPARTMENT OF DEFENSE CONTRACTORS

Aerospace Corp
ATTN: Technical Information Services
ATTN: P. Mathur

Agbabian Associates
ATTN: C. Bagge
ATTN: M. Balachanda
2 cy ATTN: M. Agbabian

Applied Theory, Inc
2 cy ATTN: J. Trulio

AVCO Research & Systems Group
ATTN: Library A630

BDM Corp
ATTN: T. Neighbors
ATTN: Corporate Library

Boeing Co
ATTN: Aerospace Library
ATTN: R. Dyrdahl
ATTN: M/S 42/37, K. Friddell
ATTN: J. Wooster
ATTN: H. Leistner
ATTN: T. Berg

California Institute of Technology
ATTN: D. Anderson

California Research & Technology, Inc
ATTN: Library
ATTN: S. Schuster
ATTN: E. Freyenhagen

California Research & Technology, Inc
ATTN: D. Orshal

University of California
ATTN: R. Goodman
ATTN: M. Cook

Calspan Corp
ATTN: Library

University of Denver
ATTN: Sec Officer for J. Wisotski

EGAG Washington Analytical Services, Inc
ATTN: Library

Electromechanical Sys of New Mexico, Inc
ATTN: R. Shunk

Eric H. Wang
Civil Engineering Dept
University of New Mexico
ATTN: G. Baum

DEPARTMENT OF DEFENSE CONTRACTORS (Continued)

Foster-Miller Associates, Inc
ATTN: J. Hampson for E. Foster

Franklin Institute
ATTN: Z. Zudans

General Electric Company—TEMPO
ATTN: DASIAC

IIT Research Institute
ATTN: R. Welch
ATTN: M. Johnson
ATTN: Documents Library

Institute for Defense Analyses
ATTN: Classified Library

J. H. Wiggins Co, Inc
ATTN: J. Collins

Kaman Avidyne
ATTN: Library

Kaman Sciences Corp
ATTN: Library

Lockheed Missiles & Space Co, Inc
ATTN: T. Geers
ATTN: Technical Information Center

Massachusetts Inst of Technology
ATTN: W. Brace

Merritt CASES, Inc
ATTN: J. Merritt

Nathan M. Newmark Consult Eng Svcs
ATTN: N. Newmark
ATTN: A. Hendron
ATTN: W. Hall

City College of New York
ATTN: C. Miller

Northwestern University
ATTN: T. Belytschko

Pacific-Sierra Research Corp
ATTN: H. Brode

Pacifica Technology
ATTN: G. Kent

Physics International Co
ATTN: Technical Library
ATTN: F. Sauer
ATTN: E. Moore

R & D Associates
ATTN: R. Port
ATTN: J. Lewis
ATTN: D. Shinivasa
ATTN: Technical Information Center
ATTN: D. Rawson
ATTN: P. Haas

DEPARTMENT OF DEFENSE CONTRACTORS (Continued)

Rand Corp
ATTN: A. Laupa

Science Applications, Inc
ATTN: Technical Library

Science Applications, Inc
ATTN: Technical Library

Science Applications, Inc
ATTN: W. Layson

Southwest Research Institute
ATTN: W. Baker
ATTN: A. Wenzel

SRI International
ATTN: B. Holmes
ATTN: H. Lindberg
ATTN: G. Abrahamson

Systems, Science & Software, Inc
ATTN: R. Duff
ATTN: D. Grine
ATTN: Library
ATTN: C. Archembeam

Terra Tek, Inc
ATTN: H. Pratt
ATTN: Library

Texas A & M University System
ATTN: J. Handin
ATTN: A. Rychlik

TRW Defense & Space Sys Group
ATTN: P. Huff
ATTN: Technical Information Center
ATTN: N. Lipner

TRW Defense & Space Sys Group
ATTN: P. Dai
ATTN: E. Wong

Universal Analytics, Inc
ATTN: E. Field

Weidlinger Assoc, Consulting Engineers
ATTN: M. Baron
ATTN: I. Sandler

Weidlinger Assoc, Consulting Engineers
ATTN: J. Isenberg

William Perret
ATTN: W. Perret